Anelastic strain recovery reveals extension across SW Japan subduction zone

Timothy B. Byrne,[1] Weiren Lin,[2] Akito Tsutsumi,[3] Yuhji Yamamoto,[4] Jonathan C. Lewis,[5] Kyuichi Kanagawa,[6] Yujin Kitamura,[7] Asuka Yamaguchi,[4] and Gaku Kimura[8]

[1] Sediment dominated convergent margins typically record substantial horizontal shortening often associated with great earthquakes. The convergent margin south of Japan is arguably one of the most extensively investigated margins and previous studies have documented extensive evidence for accretion and horizontal shortening. Here, we show results from anelastic strains recovered from three partially lithified sediment samples (∼40% porosities) across the southwest Japan accretionary prism and propose that the margin is dominated by horizontal extension rather than compression. The anelastic strain results are also consistent with stress directions interpreted from two independent techniques - bore hole breakout orientations and core-scale fault data. We interpret this unexpected result to reflect geologically recent under-thrusting of a thick sediment package and concomitant weakening of the décollément. **Citation:** Byrne, T. B., W. Lin, A. Tsutsumi, Y. Yamamoto, J. C. Lewis, K. Kanagawa, Y. Kitamura, A. Yamaguchi, and G. Kimura (2009), Anelastic strain recovery reveals extension across SW Japan subduction zone, *Geophys. Res. Lett.*, *36*, L23310, doi:10.1029/2009GL040749.

1. Introduction

[2] Establishing the *in situ* state of stress along active subduction zones is critical to understanding the accumulation and release of most of Earth's seismic energy [*Lallemand and Funiciello*, 2009]. It is also one of the main goals of the Integrated Ocean Drilling Program (IODP) as the seismogenic parts of these margins are often only accessible through drilling. Earthquake seismology has provided critical data on the orientation and magnitude of stresses along many margins at moderate to deep structural levels. In the upper few kilometers of the crust, however,

where the propagation of elastic strain released from depth can cause significant surface damage and destruction through ground shaking and tsunami generation, the state of stress is more difficult to constrain. Here, we apply the anelastic strain recovery (ASR) technique [*Lin et al.*, 2007; *Matsuki*, 1991] to whole-round sediment cores retrieved from the hanging wall of the Nankai subduction zone to constrain three-dimensional (3D) *in situ* principal stress orientations and relative magnitudes.

[3] The Nankai accretionary prism south of Kii Peninsula (Figure 1) records a long history of subduction and accretion, and remains one of the most tectonically active margins on Earth. The margin generated great earthquakes in 1944 (Mw 8.1) and 1946 (Mw 8.3) that generated tsunamis and caused significant damage in southwest Japan. Growth of the prism since at least the early Tertiary has resulted in a relatively large taper (nearly 8° [*Kimura et al.*, 2007]), suggesting that the prism is composed of relatively weak materials [*Dahlen*, 1990; *Lallemand et al.*, 1994; *Wang and Hu*, 2006]. The prism also appears to be underlain by materials with relatively low P-wave velocities that *Park et al.* [2009] (Figure 1) interpret as representing overpressured fluids. *Ito and Obara* [2006] have also recently documented a series of very low frequency earthquakes near the inferred seismic-aseismic transition and recent reinterpretation of the focal mechanisms show that they accommodate trench-parallel extension [*Ito et al.*, 2009]. A relatively large forearc basin formed about 1.7 Ma and is composed dominantly of silty clays or hemipelagic muds overlain by coarser-grained sediments [*Tobin et al.*, 2009]. Two phases of landward tilting (1.2 to 1.0 Ma and 0.4 Ma to Present) [*Expedition 315 Scientists*, 2009; *Moore et al.*, 2009] are separated by a period of sedimentation without tilting. Seismogenic motion along relatively large thrust faults, like the recently recognized "mega-splay" [*Moore et al.*, 2007; *Park et al.*, 2002], may represent this process of accretion and tilting over the period of an earthquake cycle.

2. Methods

[4] The principle idea behind the ASR technique is that stress-induced strain is released first instantaneously (i.e., as time-independent elastic strain), followed by a more gradual or time-dependent release. The ASR method takes advantage of the time-dependent strain. *Voight* [1968] first proposed that anelastic strain could provide constraints on *in situ* stress and *Matsuki* [1991] showed that the technique could be extended to 3D stress and that it could constrain stress magnitudes. The extension to 3D and stress magni-

[1]Center for Integrative Geosciences, University of Connecticut, Storrs, Connecticut, USA.

[2]Kochi Institute for Core Sample research, Japan Agency for Marine-Earth Science and Technology, Nankoku, Japan.

[3]Division of Earth and Planetary Sciences, Graduate School of Science, Kyoto University, Kyoto, Japan.

[4]Center for Advanced Marine Core Research, Kochi University, Nankoku, Japan.

[5]Department of Geoscience, Indiana University of Pennsylvania, Indiana, Pennsylvania, USA.

[6]Department of Earth Sciences, Chiba University, Chiba, Japan.

[7]Leibniz Institute of Marine Sciences at Kiel University (IFM-GEOMAR), Kiel, Germany.

[8]Department of Earth and Planetary Science, University of Tokyo, Tokyo, Japan.
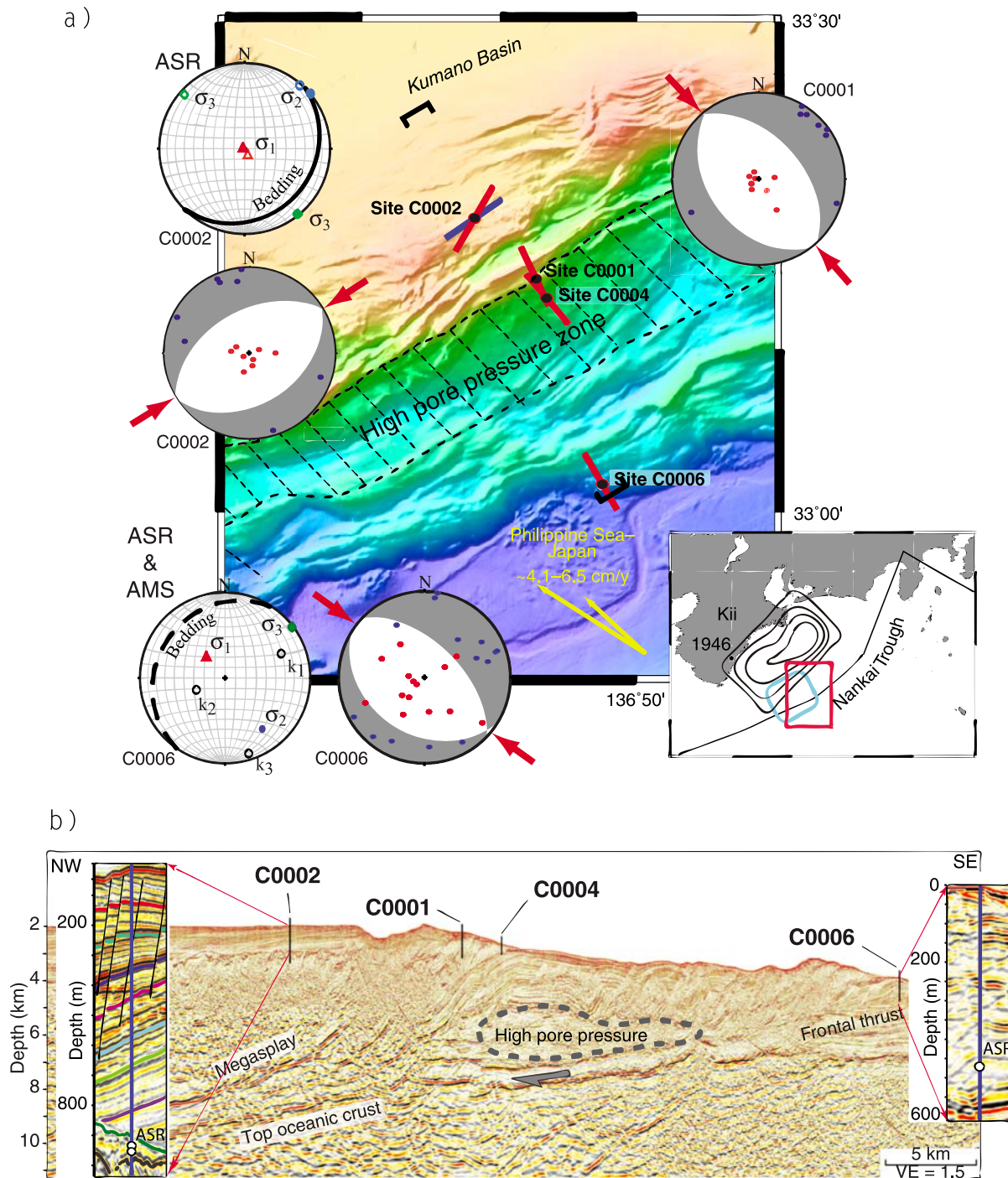
Figure 1. (a) Bathymetric map, location of IODP drilling sites and *in situ* stress results from Sites C0001, C0002, C0004 and C0006. Stereonets (lower hemisphere) show principal stress orientations from ASR data (C0002 shows results from two samples), orientation of bedding and, for C0006, the orientation of AMS axes (open circles with $k_1 > k_2 > k_3$). Short red and blue (data below 900 meters at C0002) lines at drilling sites show orientations of σ_{Hmax} from bore hole breakout data. Stereonets with shaded quadrants show "P" (red) and "T" (blue) axes from late-stage, core-scale faults; shaded areas show extension quadrants using the Bingham axial distribution statistics of the P and T axes [*Marrett and Allmendinger*, 1990]. Opposing red arrows show orientation of the intermediate axis. Brackets show location of cross-section in Figure 1b. Inset map shows 1944 earthquake epicenter and associated slip (black contours), area of very low frequency earthquakes (small blue square) [*Ito and Obara*, 2006; *Ito et al.*, 2009] and area of IODP drilling (red rectangle). (b) Seismic reflection profile [from *Moore et al.*, 2009] showing IODP drill sites along Kii transect (some sites have been projected along strike); insets show more detailed sections of Sites C0002 and C0006 with approximate locations of ASR samples. Distribution of area of high pore pressure in Figure 1b and projection to seafloor in Figure 1a are from *Park et al.* [2009].
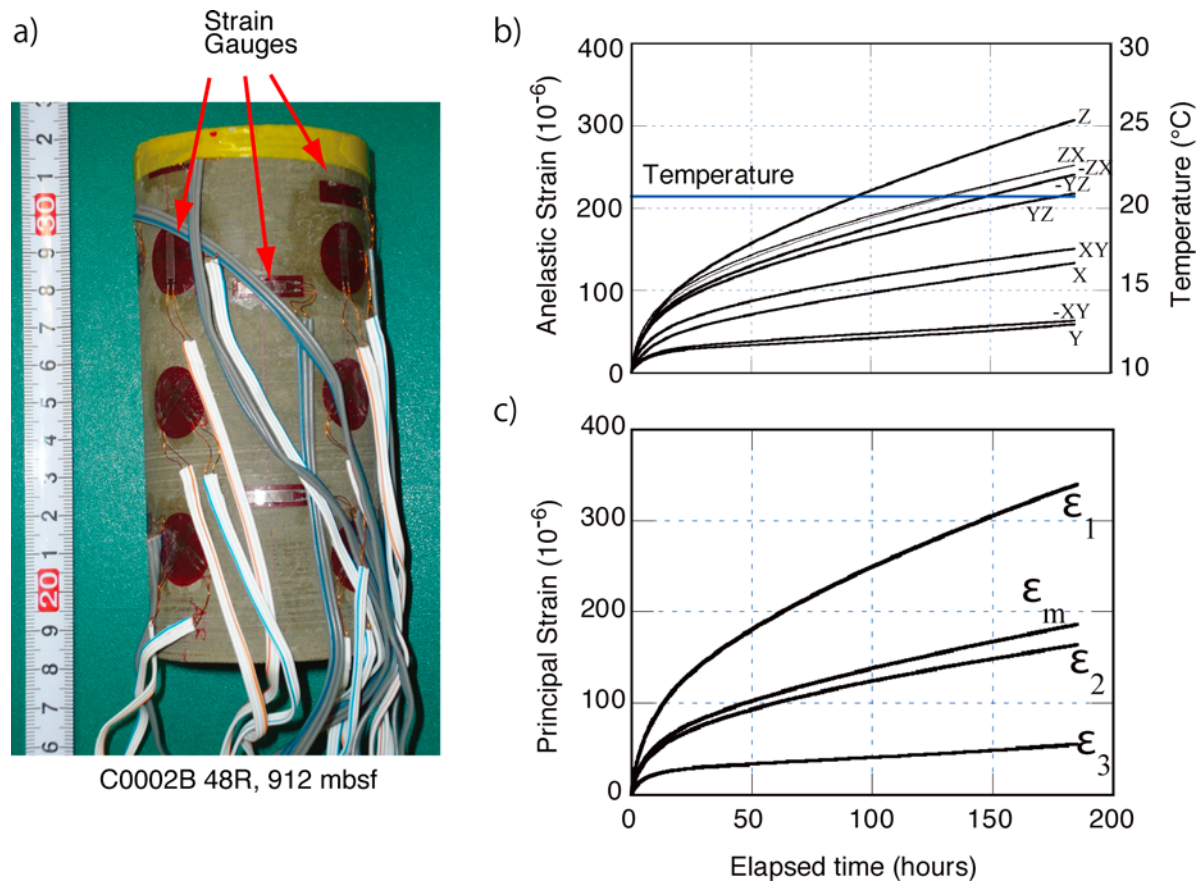
Figure 2. Results from core sample C0002B-48R-2. (a) Sample with strain gauges attached. (b) Magnitude of normal and shear strains (left axis) and temperature (right axis) versus time. (c) Magnitude of three principal strains and mean strain versus time.

tudes normally requires assuming that the rock is an isotropic and linearly viscoelastic material with two independent modes of deformation: shear and volumetric. By applying the correspondence principle of linear viscoelasticity and making the assumption that the bulk modulus of the rock matrix is not a viscoelastic parameter, *Matsuki* [1991] showed that recovered anelastic normal strain depends on the in situ stress tensor, the pore pressure and the compliances of both deformation modes. In addition, for isotropic viscoelastic materials the orientations of the three principal *in situ* stresses coincide with the orientations of the three principal anelastic strains. Thus, the orientations of the principal *in situ* stresses can be determined by calculating the orientations of principal strains based on anelastic strain data measured in at least six independent directions.

[5] Three high-quality sediment core samples (6–14 cm in length) were collected at IODP Sites C0002 (samples C0002B-45R-4 and C0002B-48R-2) and C0006 (sample C0006F-9R-1) during IODP Expeditions 315 and 316 (Figure 1) [*Ashi et al.*, 2009; *Kimura et al.*, 2009] and prepared for ASR analysis following the guidelines by *Lin et al.* [2007]. All of the samples consisted of whole-round cores of coherent silty muds of early Pliocene age with 40 to 45% porosity. Two of the samples are from the basal forearc basin (Site C0002) whereas the third sample is from a deep marine basin sequence now in the hanging wall of the

frontal thrust (C0006). After the samples were removed from the core liner, they were washed, air dried at room temperature and marked at 45° intervals to ensure that strains were measured in at least nine directions, six of which were independent. A total of eighteen gauges (Figure 2a), providing double redundancy, were connected to a digital counter that collected data every 10 minutes for up to four weeks. The samples were double bagged (clear plastic and aluminum) and submerged in a thermostatic chamber where temperature changes were controlled to less than ±0.1°C. A control sample showed that the drift of the system was very small relative to the anelastic strain of the active core samples. After data collection, all three cores were subsampled for paleomagnetic analysis. Finally, two smaller samples (10 cm^3 cubes), one about 40 cm above and the other about 60 cm below the ASR sample from Site C0006, were also collected for anisotropy of magnetic susceptibility (AMS) analysis. One of these samples was also successfully reoriented to a geographic reference frame with paleomagnetic data.

[6] The total strains in various directions ranged from about 50–300 microstrains, which is sufficiently high relative to the measurement accuracy of the system that the data can be used for a three-dimensional analysis (Figure 2b). After sufficient strain had been recovered, principal strains $\varepsilon_{1,2,3}(t)$ and the mean normal strain $\varepsilon_m(t)$

were calculated as functions of time (t) from the nine measured anelastic normal strains using a least squares analysis (Figure 2c).

3. Results

[7] All three samples yielded vertical to nearly vertical directions for the maximum principal stress, σ_1 (where $\sigma_1 > \sigma_2 > \sigma_3$) (Figure 1) and the two samples from the forearc show nearly identical orientations of σ_2 and σ_3 (Figure 1a), confirming the reliability of the ASR technique. The two forearc samples also show σ_3 (i.e., extension) normal to the trench axis, whereas the sample from the toe region of the prism shows σ_3 trench parallel (Figure 1b). In order to interpret the ASR results it is important to understand the influence of any pre-existing anisotropies, the relation between the state of stress and the strain history of the sediment, and any inconsistencies with data from other *in situ* stress techniques that are available. To this end, complementary studies were conducted during these expeditions and Expedition 314, including the analysis of (1) sediment anisotropies, (2) borehole breakouts and, (3) fault kinematics.

[8] Bedding, defined by changes in grain size or composition or a by preferred orientation of inequant grains, locally enhanced by compaction, represents the dominant fabric in the cores from Sites C0002 and C0006. Well-developed bedding fabrics (e.g., fissility), however, were only occasionally observed and the ASR samples were selected, in part, because the sediments appeared homogeneous. At C0002 3D seismic reflection data [*Moore et al.*, 2009] show bedding dipping approximately 15° southeast at the depth of the two samples from this site (Figure 1b), which is consistent with the 15° southeast dip of bedding observed in cores within a few meters of the ASR samples. Bedding is therefore slightly oblique to the principal stress plane indicated by the ASR data. P-wave velocities of sediments collected in the area of the ASR samples also indicate relatively low transverse anisotropies (e.g., ~5% to 10%) [*Expedition 314 Scientists*, 2009a] compared to the transverse strain anisotropies indicated by the ASR data (~100%). These observations and the fact that σ_1 is vertical, consistent with Anderson's theory of faulting, suggest that bedding anisotropy is a relatively minor component of the anelastic strain at this site. At C0006, bedding planes in 3D seismic reflection data [*Moore et al.*, 2009] are nearly horizontal and bedding planes in Lithologic Unit III [*Expedition 316 Scientists*, 2009], where the sample was collected, consistently show gentle dips (<30°) with dip directions ranging from west to north, which is also oblique to the principal stress planes. Bedding data closest to the sample, however, come from 35 m below the sampled interval. We therefore represent bedding in Figure 1b with a dashed line that dips gently northwest. P-wave velocity anisotropies are also relatively small at this site [*Expedition 314 Scientists*, 2009b].

[9] Tectonically induced fabrics in fine-grained sediments, like those studied here, are more subtle than bedding at the core scale and have been documented primarily through AMS data [see, e.g., *Housen et al.*, 1996; *Housen and Kanamatsu*, 2003; *Owens*, 1993]. AMS data from sediments are considered to be a measure of the penetrative fabric caused by the reorientation or redistribution of detrital grains [*Borradaile*, 1991] as the sediments are shortened and consolidated. That is, they reflect a finite amount of shortening, or strain with three orthogonal axes, k_1, k_2 and k_3, corresponding to the maximum, intermediate and minimum principal strains (i.e., elongations), respectively. In the sediments at C0006, AMS data, corrected for rotations due to drilling with paleomagnetic data, show that k_3, (maximum shortening), plunges gently southeast, nearly parallel to the plate convergent vector but orthogonal to the maximum stress indicated by the ASR data, which is steeply plunging (Figure 1a). The obliquity between the ASR and AMS axes is consistent with our interpretation that pre-existing fabrics have not influenced the ASR data significantly. We also interpret the difference between the AMS and ASR data to indicate a change from subhorizontal shortening to subvertical shortening over time. In this interpretation, the ASR data document of the current state of stress (vertical shortening) whereas the AMS data document the (finite) strain at this site (horizontal shortening), consistent with an early period of thrusting followed by normal faulting documented at this site [*Kimura et al.*, 2009]. These results also show that the ASR method is useful for extracting modern stress states in an area with a complex deformation history and in spite of probable stress cycling associated with great earthquakes.

[10] Fault kinematics based on observations of core-scale faults [*Ashi et al.*, 2009] and borehole breakout data using azimuthal resistivity images [*Tobin et al.*, 2009] from Sites C0002 and C0006 have also yielded information on the state of stress at these sites. At C0002 the trends of borehole breakouts rotate gradually clockwise with depth, forming two maxima (Figure 1). Both trends are consistent with the trends of normal faults observed in 3D seismic data in this area [*Moore et al.*, 2009] and with a narrow trench-parallel basin just seaward of this site interpreted to be at least in part extensional. Kinematic analyses of late-stage faults documented in cores from C0002 also indicate extension, and show that σ_2 trends northeast (intermediate axis, Figure 1a). Finally, the ASR data from this site show σ_1 vertical with σ_2 trending northeast (045°) consistent with the fault data and indicating that σ_{Hmax} interpreted from the borehole breakout data is σ_2.

[11] At Site C0006, borehole breakout data show σ_{Hmax} trending northwest, nearly orthogonal to the trends observed at Site C0002; similar breakout trends were observed at C0001 and C0004 (Figure 1a). Although preliminary interpretations suggested σ_{Hmax} represents σ_1 [*Tobin et al.*, 2009], a detailed kinematic analysis of late-stage faults at this site shows that σ_1 is also nearly vertical, with σ_{Hmax} representing σ_2 (Figure 1a). ASR data from C0006 are also consistent with the core-scale fault kinematics (Figure 1a). Although ASR data are not available from C0001 or C0004, fault kinematics from C0001 are similar to the results from C0006 showing a vertical σ_1 with σ_2 trending northwest (Figure 1a). Northwest striking normal faults that offset the seafloor are also visible on seismic reflection data from the area of Site C0001 [*Moore et al.*, 2009]. σ_{Hmax} axes at all

three sites, C0001, C0004 and C0006, are therefore interpreted to be σ_2 rather than σ_1.

4. Discussion

[12] Considering the tectonic setting, including several large earthquakes with thrust mechanisms, the discovery that σ_1 is vertical at several sites across the margin appears to be an anomaly. One approach to reconciling this inconsistency is to consider horizontal extension in the context of critically tapered accretionary wedges. *Wang and Hu* [2006], for example, have recently proposed a modification of the classical critical wedge theory [*Dahlen et al.*, 1984] that considers variations in stress states during and after a great earthquake. They propose that although the entire plate boundary is weak, during a large earthquake the seismogenic portion weakens further whereas the basal detachment of the outer prism strengthens, leading to deformation and shortening of the materials in the outer prism. After the earthquake, the inner wedge becomes more compressive as stress builds on the seismogenic plate boundary and the outer wedge relaxes. If the pore pressure remains high in the wedge or the basal detachment weakens, the outer wedge can become extensionally critical. This may be the case for the area off Kii Peninsula.

[13] The deformation history of the wedge over a time span greater than an earthquake cycle, however, also needs to be taken into account when constructing or evaluating orogenic models. For example, the modified critical wedge model predicts that extensional deformation, if present in either the inner or outer wedges, should alternate with compressional deformation [*Wang and Hu*, 2006]. The seaward edge of the Kumano Basin, however, is dominated by normal faults and shows little evidence of horizontal shortening. Normal faults are also consistently the youngest structures at Sites C0006 and C0001.

[14] We therefore propose the alternative hypothesis that a thick package of sediments was thrust beneath the prism relatively recently, thickening the prism and leading to fluid overpressures, a weaker decollément and a change in the state of stress. *Park et al.* [2009] have recently interpreted an extensive zone of anomalously low velocities beneath the landward half of the prism to reflect the presence of overpressured sediments (Figures 1a and 1b). Although no age data are available, the landward edge of the zone is about 30 km from the trench, suggesting that it may have been thrust beneath the prism in the last million years, assuming the present convergence rate of about 40 km/m.y. The most recent phase of landward tilting in the Kumano Basin also started about a half a million years ago and was preceded by a period of relatively rapid sedimentation ($\sim$400 m/1000 yr), starting about 1.7 Ma [*Ashi et al.*, 2009]. Rapid sedimentation followed by underthrusting of a thick pile of sediment may have both thickened the prism, increasing the taper angle, and weakened the decollément, leading to lower (tectonic) horizontal stresses and/or higher vertical stresses in the hanging wall.

[15] The change in orientation of σ_2 across the prism from northeast trending at Site C0002 to northwest trending elsewhere apparently reflects the increase in importance of horizontal compression near the plate boundary (i.e., the Nankai Trough). That is, σ_2 in this area represents the plate

tectonic stress although it is smaller in magnitude than the vertical stress. Presumably, at some depth below the depths sampled during Expeditions 315 and 316, plate tectonic stresses dominate and σ_1 approaches horizontal [see e.g., *Ito et al.*, 2009].

[16] In summary, anelastic strains recovered from three partially lithified sediment samples ($\sim$40% porosities) across the Nankai accretionary prism are consistent with stress directions interpreted from two independent techniques - bore hole breakout orientations and core-scale fault data. The ASR principal strain axes at both sites are also oblique to bedding and, at C0006, are oblique to fabrics defined by AMS. The AMS fabrics dip steeply consistent with horizontal tectonic stresses and shortening. Based on the pervasive occurrence of late-stage normal faults and the ASR data, we interpret the AMS data to reflect remnant fabrics from an earlier phase of shortening. Stresses across this region of the prism today are dominantly extensional (i.e., maximum principal stress is vertical) in at least the upper structural levels. We propose that the current state of stress reflects the relatively recent (<1 million years) underthrusting of a thick sediment pile that weakened the decollément.

References

Ashi, J., et al. (2009), Expedition 315 summary, in *NanTroSEIZE Stage 1: Investigations of Seismogenesis, Nankai Trough, Japan, Proc. Integr. Ocean Drill. Program, 314/315/316*, doi:10.2204/iodp.proc.314315316.121.2009.

Borradaile, G. (1991), Correlation of strain with anisotropy of magnetic-susceptibility (AMS), *Pure Appl. Geophys., 135*, 15–29, doi:10.1007/BF00877006.

Dahlen, F. A. (1990), Critical taper model of fold-and-thrust belts and accretionary wedges, *Annu. Rev. Earth Planet. Sci., 18*, 55–99, doi:10.1146/annurev.ea.18.050190.000415.

Dahlen, F. A., J. Suppe, and D. Davis (1984), Mechanics of fold-and-thrust belts and accretionary wedges: Cohesive Coulomb theory, *J. Geophys. Res., 89*, 10,087–10,101, doi:10.1029/JB089iB12p10087.

Expedition 314 Scientists (2009a), Expedition 314 Site C0002, in *NanTroSEIZE Stage 1: Investigations of Seismogenesis, Nankai Trough, Japan, Proc. Integr. Ocean Drill. Program, 314/315/316*, doi:10.2204/iodp.proc.314315316.114.2009.

Expedition 314 Scientists (2009b), Expedition 314 Site C0006, in *NanTroSEIZE Stage 1: Investigations of Seismogenesis, Nankai Trough, Japan, Proc. Integr. Ocean Drill. Program, 314/315/316*, doi:10.2204/iodp.proc.314315316.118.2009.

Expedition 315 Scientists (2009), Expedition 315 Site C0002, in *NanTroSEIZE Stage 1: Investigations of Seismogenesis, Nankai Trough, Japan, Proc. Integr. Ocean Drill. Program, 314/315/316*, doi:10.2204/iodp.proc.314315316.124.2009.

Expedition 316 Scientists (2009), Expedition 316 Site C0006, in *NanTroSEIZE Stage 1: Investigations of Seismogenesis, Nankai Trough, Japan, Proc. Integr. Ocean Drill. Program, 314/315/316*, doi:10.2204/iodp.proc.314315316.134.2009.

Housen, B. A., and T. Kanamatsu (2003), Magnetic fabrics from the Costa Rica margin: Sediment deformation during the initial dewatering and underplating process, *Earth Planet. Sci. Lett., 206*, 215–228, doi:10.1016/S0012-821X(02)01076-2.

Housen, B. A., et al. (1996), Strain decoupling across the Barbados accretionary prism, *Geology, 24*, 127–130, doi:10.1130/0091-7613(1996)024<0127:SDATDO>2.3.CO;2.

Ito, Y., and K. Obara (2006), Dynamic deformation of the accretionary prism excites very low frequency earthquakes, *Geophys. Res. Lett.*, *33*, L02311, doi:10.1029/2005GL025270.

Ito, Y., Y. Asano, and K. Obara (2009), Very-low-frequency earthquakes indicate a transpressional stress regime in the Nankai accretionary prism, *Geophys. Res. Lett.*, *36*, L20309, doi:10.1029/2009GL039332.

Kimura, G., et al. (2007), Transition of accretionary wedge structures around the up-dip limit of the seismogenic subduction zone, *Earth Planet. Sci. Lett.*, *255*, 471–484, doi:10.1016/j.epsl.2007.01.005.

Kimura, G., et al. (2009), Expedition 316 summary, in *NanTroSEIZE Stage 1: Investigations of Seismogenesis, Nankai Trough, Japan*, *Proc. Integr. Ocean Drill. Program*, *314/315/316*, doi:10.2204/iodp.proc.314315316.131.2009.

Lallemand, S., and F. Funiciello (2009), *Subduction Zone Geodynamics*, Springer, Berlin.

Lallemand, S. E., P. Schnürle, and J. Malavieille (1994), Coulomb theory applied to accretionary and nonaccretionary wedges: Possible causes for tectonic erosion and/or frontal accretion, *J. Geophys. Res.*, *99*, 12,033–12,055, doi:10.1029/94JB00124.

Lin, W., et al. (2007), Preliminary results of stress measurements using drill cores of TCDP Hole-A: An application of anelastic strain recovery method to three-dimensional in-situ stress determination, *Terr. Atmos. Oceanic Sci.*, *18*, 379–393.

Marrett, R., and R. W. Allmendinger (1990), Kinematic analysis of fault-slip data, *J. Struct. Geol.*, *12*, 973–986, doi:10.1016/0191-8141(90)90093-E.

Matsuki, K. (1991), Three-dimensional in-situ stress measurement with anelastic strain recovery of a rock core, in *Proceedings of the 7th International Congress on Rock Mechanics*, edited by W. Wittke, pp. 557–560, Taylor and Francis, London.

Moore, G., et al. (2007), Three-dimensional spaly fault geometry and implications for tsunami generation, *Science*, *318*, 1128–1131, doi:10.1126/science.1147195.

Moore, G. F., et al. (2009), Structural and seismic stratigraphic framework of the NanTroSEIZE Stage 1 transect, in *NanTroSEIZE Stage 1: Investigations of Seismogenesis, Nankai Trough, Japan*, *Proc. Integr. Ocean Drill. Program*, *314/315/316*, doi:10.2204/iodp.proc.314315316.102.2009.

Owens, W. (1993), Remanence and magnetic fabric studies of samples from Hole 131-808C, Nankai, Trough, *Proc. Ocean Drill. Program Sci. Results*, *131*, 301–310.

Park, J.-O., et al. (2002), Splay fault branching along the Nankai subduction zone, *Science*, *297*, 1157–1160, doi:10.1126/science.1074111.

Park, J.-O., et al. (2009), A low velocity zone with weak reflectivity along the Nankai subduction zone, *Geology*, in press.

Tobin, H., et al. (2009), Expedition 314 summary, in *NanTroSEIZE Stage 1: Investigations of Seismogenesis, Nankai Trough, Japan*, *Proc. Integr. Ocean Drill. Program*, *314/315/316*, doi:10.2204/iodp.proc.314315316.111.2009.

Voight, B. (1968), Determination of the virgin state of stress in the vicinity of a borehole from measurements of a partial anelastic strain tensor in drill cores, *Felsmech. Ingenieurgeol.*, *6*, 201–215.

Wang, K., and Y. Hu (2006), Accretionary prisms in subduction earthquake cycles: The theory of dynamic Coulomb wedge, *J. Geophys. Res.*, *111*, B06410, doi:10.1029/2005JB004094.

─────────────

T. B. Byrne, Center for Integrative Geosciences, University of Connecticut, 354 Mansfield Rd., Storrs, CT 06269, USA. (tim.byrne@uconn.edu)

K. Kanagawa, Department of Earth Sciences, Chiba University, Chiba 263-8522, Japan. (kyu_kanagawa@faculty.chiba-u.jp)

G. Kimura, Department of Earth and Planetary Science, University of Tokyo, 7-3-1 Hongo, Bunkyo-ku, Tokyo 113-0033, Japan. (gaku@eps.s.u-tokyo.ac.jp)

Y. Kitamura, Leibniz Institute of Marine Sciences at Kiel University (IFM-GEOMAR), Wischhofstrasse 1-3, D-24148 Kiel, Germany. (ykitamura@ifm-geomar.de)

J. C. Lewis, Department of Geoscience, Indiana University of Pennsylvania, 114 Walsh Hall, Indiana, PA 15705, USA. (jclewis@iup.edu)

W. Lin, Kochi Institute for Core Sample research, Japan Agency for Marine-Earth Science and Technology, 200 Monobe-otsu, Nankoku, Kochi 783-8502, Japan. (lin@jamstec.go.jp)

A. Tsutsumi, Division of Earth and Planetary Sciences, Graduate School of Science, Kyoto University, Kyoto 606-8502, Japan. (tsutsumi@kueps.kyoto-u.ac.jp)

A. Yamaguchi and Y. Yamamoto, Center for Advanced Marine Core Research, Kochi University, 200 Monobe-otsu, Nankoku, Kochi 783-8502, Japan. (jm-asukay@kochi-u.ac.jp; y.yamamoto@kochi-u.ac.jp)